Received: 26 April 2018 | Revised: 4 July 2018 | Accepted: 6 July 2018

DOI: 10.1002/bit.26789

ARTICLE

WILEY BIOTECHNOLOGY BIOENGINEERING

Metabolic engineering of *Bacillus subtilis* for L-valine overproduction

Adam W. Westbrook | Xiang Ren | Murray Moo-Young | C. Perry Chou

Department of Chemical Engineering, University of Waterloo, Waterloo, Ontario, Canada

Correspondence
C. Perry Chou, Department of Chemical Engineering, University of Waterloo, Waterloo, Ontario, Canada N2L 5B6.
Email: cpchou@uwaterloo.ca

Funding information
Natural Sciences and Engineering Research Council of Canada, Grant/Award Number: CRC 950-211471

Abstract

Bacillus subtilis has been commonly applied to industrial enzyme production due to its genetic tractability, "generally recognized as safe (GRAS)" status, and robust growth characteristics. In spite of its ideal attributes as a biomanufacturing platform, *B. subtilis* has seen limited use in the production of other value-added biochemicals. Here, we report the derivation of engineered strains of *B. subtilis* for L-valine overproduction using our recently developed CRISPR (clustered regularly interspaced palindromic repeats)-Cas9 (CRISPR-associated [protein] 9) toolkit. We first manipulate the native L-valine biosynthetic pathway by relieving transcriptional and allosteric regulation, resulting in a >14-fold increase in the L-valine titer, compared to the wild-type strain. We subsequently identify and eliminate factors limiting L-valine overproduction, specifically increasing pyruvate availability and blocking the competing L-leucine and L-isoleucine biosynthetic pathways. By inactivating (a) *pdhA*, encoding the E1α subunit of the pyruvate dehydrogenase complex, to increase the intracellular pyruvate pool, and (b) *leuA* and *ilvA*, respectively encoding 2-isopropylmalate synthase and L-threonine dehydratase, to abolish the competing pathways, the L-valine titer reached 4.61 g/L in shake flask cultures. Our engineered L-valine-overproducing strains of *B. subtilis* are devoid of plasmids and do not sporulate due to the inactivation of *sigF*, encoding the sporulation-specific transcription factor σ^F, making them attractive for large-scale L-valine production. However, acetate dissimilation was identified as limiting L-valine overproduction in Δ*pdhA B. subtilis* strains, and improving acetate dissimilation or identifying alternate modes of increasing pyruvate pools to enhance L-valine-overproduction should be explored.

KEYWORDS
amino acids, *Bacillus subtilis*, CRISPR, L-valine, metabolic engineering, synthetic biology

1 | INTRODUCTION

As one of the three branched-chain amino acids (BCAAs), L-valine is an essential nutrient for humans and animals. It is used in infusion solutions and human dietary supplements (Karau & Grayson, 2014), commercial feed in the swine and poultry industries (Oldiges, Eikmanns, & Blombach, 2014), and as a precursor for herbicide and antibiotic synthesis (Oldiges et al., 2014). Traditional extraction of L-valine, and most other amino acids, from protein hydrolysate has been replaced by microbial production and/or enzymatic synthesis (Xie, Liang, Huang, & Xu, 2014). To date, *Escherichia coli* (Park, Jang, Lee, & Lee, 2011; Park, Kim, Lee, & Lee, 2011; Park, Lee, Kim, & Lee, 2007) and *Corynebacterium glutamicum* (Blombach, Schreiner, Bartek, Oldiges, & Eikmanns, 2008; Chen, Li, Hu, Dong, & Wang, 2015; Elišáková et al., 2005; Hasegawa et al., 2013; Radmacher et al., 2002) have been extensively engineered for microbial L-valine overproduction. Given the current popularity of *C. glutamicum* as a workhorse for industrial amino acid production (Yang et al., 2015), other promising

microorganisms are also under active exploration. Among these alternatives, *Bacillus subtilis* is a genetically tractable model Gram-positive bacterium, grows rapidly in simple medium, and has been granted generally recognized as safe (GRAS) status (Schallmey, Singh, & Ward, 2004). Moreover, a comprehensive CRISPR (clustered regularly interspaced palindromic repeats)-Cas9 (CRISPR-associated [protein] 9) toolkit was recently developed for *B. subtilis*, enabling efficient genome editing, multiplexing of gene mutations, and transcriptional repression (Westbrook, Moo-Young, & Chou, 2016), such that scalable strain construction can now be achieved for this microorganism. Practically, *B. subtilis* serves as a biomanufacturing platform for the commercial production of enzymes (Westers, Westers, & Quax, 2004), hyaluronic acid (Liu, Liu, Li, Du, & Chen, 2011), and surfactants (Yoneda, Miyota, Furuya, & Tsuzuki, 2006). These various technological advantages suggest the potential of using *B. subtilis* as a host for the production amino acids, such as L-valine in this study. Note that *B. subtilis* is capable of high-level isobutanol production (Li, Huang, Li, Wen, & Jia, 2012), with which the L-valine biosynthetic pathway shares the common precursor 2-ketoisovalerate.

Like many important biomolecules, BCAAs are derived from pyruvate and their biosynthesis is controlled at the transcriptional level through a complex regulatory cascade in *B. subtilis*. Pyruvate is first converted to 2-acetolactate as an intermediate of L-valine biosynthesis by an acetohydroxy-acid synthase (AHAS) composed of regulatory (i.e., IlvH, encoded by *ilvH*) and catalytic (i.e., IlvB, encoded by *ilvB*) subunits, or by acetolactate synthase (ALS) encoded by *alsS* (AlsS; Figure 1). In parallel, IlvBH can convert 2-ketobutyrate (derived from L-threonine) and pyruvate to 2-aceto-2-hydroxybutyrate as an intermediate of L-isoleucine biosynthesis (Figure 1; Chipman, Ze, & Schloss, 1998). On the other hand, AlsS appears to be a dedicated enzyme as it is only involved in L-valine, but not L-isoleucine, synthesis (Renna, Najimudin, Winik, & Zahler, 1993). This is a common characteristic of several bacterial ALSs that convert pyruvate to 2-acetolactate as a precursor to acetoin production (Chipman et al., 1998; Renna et al., 1993). 2-Acetolactate and 2-aceto-2-hydroxybutyrate are respectively converted to 2,3-dihydroxyisovalerate and 2,3-dihydroxy-3-methylpentanoate by acetohydroxy-acid isomeroreductase (i.e., IlvC, encoded by *ilvC*), followed by their conversion to 2-ketoisovalerate and 3-methyl-2-oxopentanoate, respectively, by dihydroxy-acid dehydratase (i.e., IlvD, encoded by *ilvD*; Figure 1). Finally, 2-ketoisovalerate and 3-methyl-2-oxopentanoate are converted to L-valine and L-isoleucine, respectively, by one of two BCAA aminotransferases, that is, YbgE (encoded by *ybgE*) and YwaA (encoded by *ywaA*), either of which can also convert 4-methyl-2-oxopentanoate to L-leucine (Figure 1).

In *B. subtilis*, the genes comprising the biosynthetic pathways of BCAAs are organized into five operons: (a) *ilvBHC-leuABCD* (*leuABCD* encodes 2-isopropylmalate synthase, 3-isopropylmalate dehydrogenase, and 2-isopropylmalate dehydratase large and small subunits, respectively); (b) *ilvA* (encoding L-threonine dehydratase); (c) *ilvD*; (d) *ybgE*; and (e) *ywaA* (Mäder, Hennig, Hecker, & Homuth, 2004). All of these operons are repressed under amino-acid-rich conditions by the activity of the transcriptional regulator CodY (Brinsmade et al., 2014; Molle et al., 2003; Sonenshein, 2007), and L-valine and L-isoleucine are positive effectors of CodY such that BCAA biosynthesis is negatively autoregulated at relatively low BCAA concentrations (Sonenshein, 2007). Specifically, expression of the *ilvBHC-leuABCD* (*ilv-leu*) operon is repressed through the interaction of CodY with two high-affinity (i.e., CodY-I and CodY-II) and two low-affinity (i.e., CodY-III and CodY-IV) binding sites associated with promoter $P_{ilv\text{-}leu}$. In addition, a T-box serves as a transcription termination signal unless it is bound by uncharged $tRNA^{Leu}$, providing additional transcriptional regulation of the *ilv-leu* operon in the presence of excess L-leucine (Grandoni, Fulmer, Brizzio, Zahler, & Calvo, 1993). The CodY binding sites regulating the expression of *ilvA* and *ybgE* have been partially identified (two proposed upstream sites each), and those of *ilvD* and *ywaA* have been spatially defined (one upstream site each) via in vitro DNA affinity purification sequencing (IDAP-Seq; Belitsky & Sonenshein, 2013).

On the other hand, L-valine biosynthesis can be potentially affected by acetoin formation (Figure 1), which is associated with the expression of the *alsSD* operon. The *alsSD* operon is expressed during anaerobic fermentative growth, or under aerobic conditions as cells enter the stationary phase or during exponential growth under high glucose concentrations (Frädrich et al., 2012; Renna et al., 1993). The transcriptional regulator AlsR, encoded by *alsR*, activates transcription of *alsSD* from promoter P_{alsSD} in response to the accumulation of its presumed inducer, acetate, and *alsR* is transcribed divergently from *alsSD* from the promoter adjacent to P_{alsSD}, that is, P_{alsR} (Frädrich et al., 2012). In addition, the transcriptional repressor Rex may repress transcription from P_{alsSD} in response to low NADH levels via a putative Rex binding site that has not been formally identified (Reents, Münch, Dammeyer, Jahn, & Härtig, 2006).

Once L-valine has been synthesized in *B. subtilis*, it can be utilized for protein synthesis, secreted from the cell, or converted back to 2-ketoisovalerate as an intermediate in the synthesis of branched-chain fatty acids, the major acyl constituents of the cell membrane (Debarbouille, Gardan, Arnaud, & Rapoport, 1999). The contribution of various permeases BcaP, BraB, and BrnQ to BCAA uptake has been investigated, and BcaP, encoded by *bcaP*, appears to be the most efficient permease for the uptake of L-valine and L-isoleucine (Belitsky, 2015). Hence, it may be the most effective transporter for secretion of excess L-valine out of *B. subtilis*. The expression of *bcaP* from promoter P_{bcaP} is strongly repressed by CodY in amino-acid-rich medium via two CodY binding sites, that is, CodY-I and CodY-II (Belitsky & Sonenshein, 2011). The conversion of L-valine to 2-ketoisovalerate as the first step of the L-valine degradation pathway is potentially catalyzed by YbgE, YwaA, or Bcd (i.e., BCAA dehydrogenase, encoded by *bcd*). Relatively small decreases in CodY activity can significantly increase the expression of *bcd* and *ywaA*, compared to the expression of *ybgE*, which occurs when CodY is almost completely inactive (Brinsmade et al., 2014). Speculation has been made that the coexpression of YwaA and Bcd when CodY is largely active may indicate that both enzymes primarily convert BCAAs to their corresponding branched-chain keto acids (BCKAs),

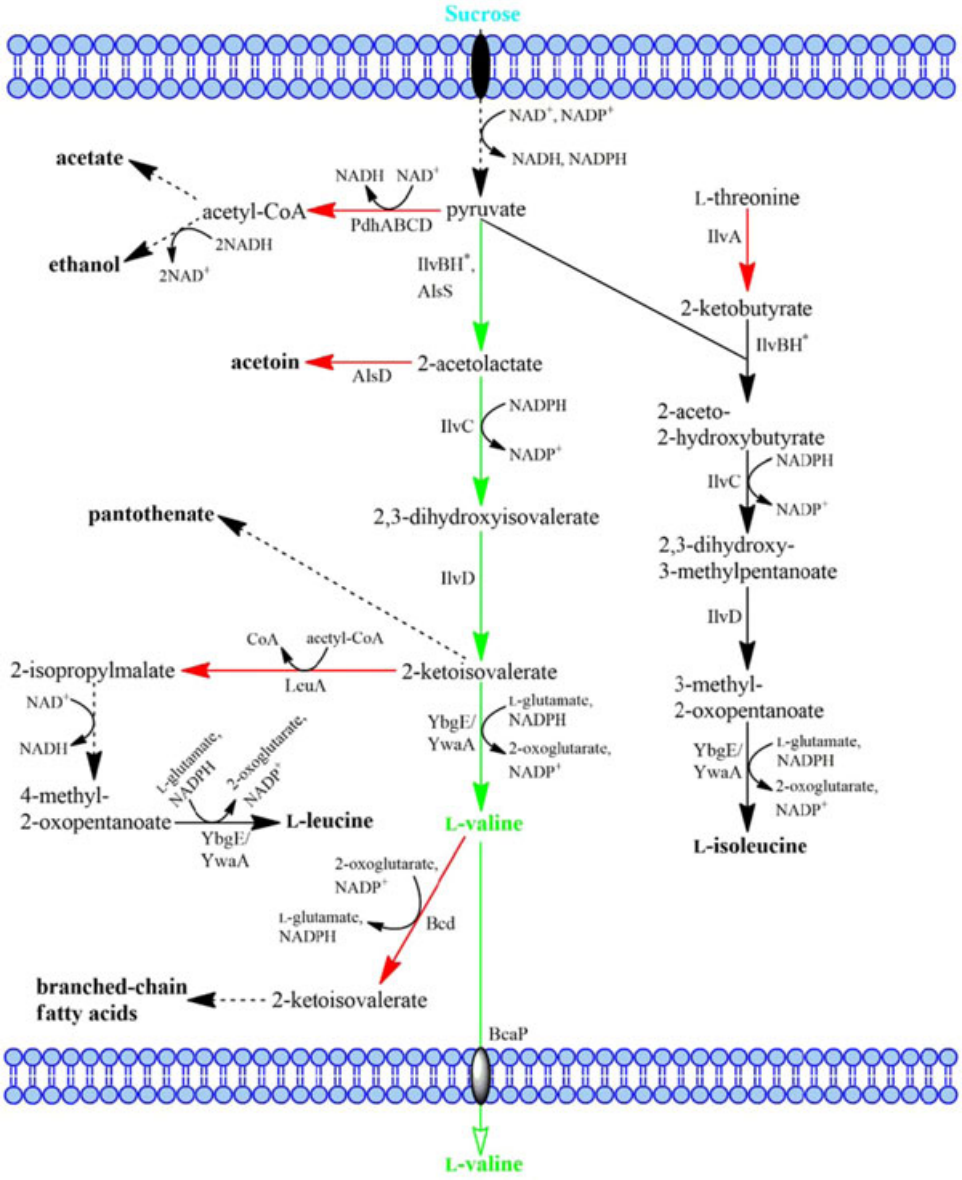

FIGURE 1 The L-valine biosynthetic pathway in *B. subtilis*. Green arrows represent reactions catalyzed by enzymes whose expression was upregulated, and red arrows represent reactions catalyzed by enzymes that were inactivated. AlsS: acetolactate synthase; BcaP: BCAA permease; Bcd: BCAA dehydrogenase; IlvA: L-threonine dehydratase; IlvB: acetohydroxy-acid synthase catalytic subunit; IlvC: acetohydroxy-acid isomeroreductase; IlvD: dihydroxy-acid dehydratase; IlvH*: engineered acetohydroxy-acid synthase regulatory subunit; LeuA: 2-isopropylmalate synthase; PdhABCD: pyruvate dehydrogenase complex; YbgE: BCAA aminotransferase; YwaA: BCAA aminotransferase [Color figure can be viewed at wileyonlinelibrary.com]

while YbgE converts BCKAs to BCAAs upon nutrient limitation (Brinsmade et al., 2014). However, the mutation of *bcd* completely abolished the growth of *B. subtilis* when L-valine and L-isoleucine were supplied as the sole nitrogen source (Debarbouille et al., 1999), suggesting that YwaA does not naturally play a role in BCAA catabolism.

While *B. subtilis* has been used extensively in biomanufacturing as previously outlined, it is not commonly used as a host for amino acid production. In this study, we engineered the metabolism of *B. subtilis* for L-valine overproduction using our recently developed CRISPR-Cas9 toolkit (Westbrook et al., 2016). The L-valine titer was increased by >14-fold, compared to the wild-type strain, by manipulating the $P_{ilv\text{-}leu}$ promoter and its regulatory elements, engineering IlvH to reduce L-valine feedback inhibition, chromosomally overexpressing *ilvD*, *ybgE*, and *ywaA* to enhance biosynthetic pathway toward L-valine, and mutating *bcd* to block L-valine degradation. Further investigation revealed that pyruvate availability was critically limiting L-valine overproduction in our engineered strains, and this was overcome by mutating *pdhA*, encoding the E1α subunit (PdhA) of the pyruvate dehydrogenase complex (PdhABCD), further increasing the L-valine titer. Moreover, inactivation of the L-leucine and L-isoleucine biosynthetic pathways via mutation of *leuA* and *ilvA*, respectively, in the Δ*pdhA* background further improved L-valine overproduction, resulting in a titer of 4.61 g/L in shake flask cultures. In addition, our

TABLE 1 Strains and plasmids used in this study

Strain or plasmid	Characteristics[a]	Source
E. coli		
HI-Control™ 10G	*mcrA* Δ(*mrr-hsdRMS-mcrBC*) *endA1 recA1* ϕ80d*lacZ*ΔM15 Δ*lacX74 araD139* Δ(*ara, leu*)*7697galU galK rpsL* (StrR) *nupG* λ− *tonA* Mini-F *lacIq1* (Gent^R)	Lucigen
B. subtilis		
1A751	*his npr* R2 *npr*E18 Δ*aprA*3 Δ*eglS*102 Δ*bglT bglS* RV	Wolf, Geczi, Simon, and Borriss (1995)
AW001-2	1A751 *lacA*::(*cas9*, tracrRNA, Erm^R)	Westbrook et al. (2016)
AW001-5	1A751 *lacA*::(*cas9*, tracrRNA, Erm^R), *bpr*::($P_{xylA,\ Bm}$::*comK*:*comS*, *xylR*)	This study
AW002-5	1A751 *lacA*::(*cas9*, tracrRNA, Erm^R), *bpr*::($P_{xylA,\ Bm}$::*comK*:*comS*, *xylR*), P_{grac}::*ilvBHC*, Δ*bcd*	This study
AW003-5	1A751 *lacA*::(*cas9*, tracrRNA, Erm^R), *bpr*::($P_{xylA,\ Bm}$::*comK*:*comS*, *xylR*), P_{grac}::*ilvBHC*, Δ*bcd*, *amyE*::P_{grac}::*ybgE*:*ywaA*	This study
AW004-5	1A751 *lacA*::(*cas9*, tracrRNA, Erm^R), *bpr*::($P_{xylA,\ Bm}$::*comK*:*comS*, *xylR*), P_{grac}::*ilvBHC*, Δ*bcd*, *amyE*::P_{grac}::*ybgE*:*ywaA*, *wprA*::P_{grac}::*ilvD*	This study
AW005-5	1A751 *lacA*::(*cas9*, tracrRNA, Erm^R), *bpr*::($P_{xylA,\ Bm}$::*comK*:*comS*, *xylR*), P_{grac}::*ilvBH*C*, Δ*bcd*, *amyE*::P_{grac}::*ybgE*:*ywaA*, *wprA*::P_{grac}::*ilvD*	This study
AW006-5	1A751 *lacA*::(*cas9*, tracrRNA, Erm^R), *bpr*::($P_{xylA,\ Bm}$::*comK*:*comS*, *xylR*), P_{grac}::*ilvBHC*, Δ*bcd*, *amyE*::P_{grac}::*ybgE*:*ywaA*, *wprA*::P_{grac}::*ilvD*, $P_{grac.UPmod}$::*alsSD*, Δ*ilvB*	This study
AW007-5	1A751 *lacA*::(*cas9*, tracrRNA, Erm^R), *bpr*::($P_{xylA,\ Bm}$::*comK*:*comS*, *xylR*), P_{grac}::*ilvBH*C*, Δ*bcd*, *amyE*::P_{grac}::*ybgE*:*ywaA*, *wprA*::P_{grac}::*ilvD*, Δ*leuA*, Δ*ilvA*	This study
AW008-5	1A751 *lacA*::(*cas9*, tracrRNA, Erm^R), *bpr*::($P_{xylA,\ Bm}$::*comK*:*comS*, *xylR*), P_{grac}::*ilvBH*C*, Δ*bcd*, *amyE*::P_{grac}::*ybgE*:*ywaA*, *wprA*::P_{grac}::*ilvD*, Δ*leuA*, Δ*ilvA*, $P_{grac.UPmod}$::*alsSD*	This study
AW009-5	1A751 *lacA*::(*cas9*, tracrRNA, Erm^R), *bpr*::($P_{xylA,\ Bm}$::*comK*:*comS*, *xylR*), P_{grac}::*ilvBH*C*, Δ*bcd*, *amyE*::P_{grac}::*ybgE*:*ywaA*, *wprA*::P_{grac}::*ilvD*, Δ*leuA*, Δ*ilvA*, P_{mtlA}::*alsSD*	This study
AW010-5	1A751 *lacA*::(*cas9*, tracrRNA, Erm^R), *bpr*::($P_{xylA,\ Bm}$::*comK*:*comS*, *xylR*), P_{grac}::*ilvBH*C*, Δ*bcd*, *amyE*::P_{grac}::*ybgE*:*ywaA*, *wprA*::P_{grac}::*ilvD*, Δ*leuA*, Δ*ilvA*, P_{mtlA}::*alsSD*, Δ*alsD*	This study
AW011-5	1A751 *lacA*::(*cas9*, tracrRNA, Erm^R), *bpr*::($P_{xylA,\ Bm}$::*comK*:*comS*, *xylR*), P_{grac}::*ilvBH*C*, Δ*bcd*, *amyE*::P_{grac}::*ybgE*:*ywaA*, *wprA*::P_{grac}::*ilvD*, Δ*leuA*, Δ*ilvA*, P_{mtlA}::*als*, Δ*alsD*, $P_{grac.UPmod}$::*bcaP*	This study
AW012-5	1A751 *lacA*::(*cas9*, tracrRNA, Erm^R), *bpr*::($P_{xylA,\ Bm}$::*comK*:*comS*, *xylR*), P_{grac}::*ilvBH*C*, Δ*bcd*, *amyE*::P_{grac}::*ybgE*:*ywaA*, *wprA*::P_{grac}::*ilvD*, Δ*leuA*, Δ*ilvA*, P_{mtlA}::*als*, Δ*alsD*, $P_{grac.UPmod}$::*bcaP*, Δ*pdhA*	This study
AW013-5	1A751 *lacA*::(*cas9*, tracrRNA, Erm^R), *bpr*::($P_{xylA,\ Bm}$::*comK*:*comS*, *xylR*), P_{grac}::*ilvBHC*, Δ*bcd*, *amyE*::P_{grac}::*ybgE*:*ywaA*, *wprA*::P_{grac}::*ilvD*, Δ*pdhA*	This study
AW014-5	1A751 *lacA*::(*cas9*, tracrRNA, Erm^R), *bpr*::($P_{xylA,\ Bm}$::*comK*:*comS*, *xylR*), P_{grac}::*ilvBH*C*, Δ*bcd*, *amyE*::P_{grac}::*ybgE*:*ywaA*, *wprA*::P_{grac}::*ilvD*, Δ*pdhA*	This study
AW015-5	1A751 *lacA*::(*cas9*, tracrRNA, Erm^R), *bpr*::($P_{xylA,\ Bm}$::*comK*:*comS*, *xylR*), P_{grac}::*ilvBH*C*, Δ*bcd*, *amyE*::P_{grac}::*ybgE*:*ywaA*, *wprA*::P_{grac}::*ilvD*, Δ*leuA*, Δ*ilvA*, Δ*pdhA*	This study
AW016-5	1A751 *lacA*::(*cas9*, tracrRNA, Erm^R), *bpr*::($P_{xylA,\ Bm}$::*comK*:*comS*, *xylR*), P_{grac}::*ilvBH*C*, Δ*bcd*, *amyE*::P_{grac}::*ybgE*:*ywaA*, *wprA*::P_{grac}::*ilvD*, Δ*leuA*, Δ*ilvA*, P_{mtlA}::*alsSD*, Δ*pdhA*	This study
AW017-5	1A751 *lacA*::(*cas9*, tracrRNA, Erm^R), *bpr*::($P_{xylA,\ Bm}$::*comK*:*comS*, *xylR*), P_{grac}::*ilvBH*C*, Δ*bcd*, *amyE*::P_{grac}::*ybgE*:*ywaA*, *wprA*::P_{grac}::*ilvD*, Δ*leuA*, Δ*ilvA*, P_{mtlA}::*alsSD*, Δ*alsD*, Δ*pdhA*	This study
AW018-5	1A751 *lacA*::(*cas9*, tracrRNA, Erm^R), *bpr*::($P_{xylA,\ Bm}$::*comK*:*comS*, *xylR*), P_{grac}::*ilvBH*C*, Δ*bcd*, *amyE*::P_{grac}::*ybgE*:*ywaA*, *wprA*::P_{grac}::*ilvD*, Δ*leuA*, Δ*ilvA*, Δ*pdhA*, Δ*sigF*	This study
AW019-5	1A751 *lacA*::(*cas9*, tracrRNA, Erm^R), *bpr*::($P_{xylA,\ Bm}$::*comK*:*comS*, *xylR*), P_{grac}::*ilvBHC*, Δ*bcd*, *amyE*::P_{grac}::*ybgE*:*ywaA*, *wprA*::P_{grac}::*ilvD*, Δ*pdhA*, Δ*leuA*, Δ*ilvA*	This study
Plasmids		
pAX01	$P_{xylA,\ Bm}$, *xylR*, Amp^R, Erm^R, *B. subtilis lacA* integration vector	Härtl, Wehrl, Wiegert, Homuth, and Schumann (2001)

(Continues)

TABLE 1 (Continued)

Strain or plasmid	Characteristics[a]	Source
pgRNA-bacteria	*E. coli* plasmid for gRNA transcription	Qi et al. (2013)
pAW008	P_{grac}::*seHas*:*tuaD*, Neo^R, *B. subtilis amyE* integration vector	Westbrook et al. (2016)
pAW004-2	P_{araE}::*mazF*, *araR*, Spc^R, Erm^R, *B. subtilis* auto-evicting counter-selectable *thrC* integration vector	Westbrook et al. (2016)
pAW014-2	(*Bgl*II) $P_{xylA.SphI+1}$::*ugtP*-gRNA.P395T (*Nco*I), P_{araE}::*mazF*, *araR*, Spc^R, Erm^R, *B. subtilis* multi-gRNA counter-selectable *thrC* integration vector	Westbrook et al. (2016)
pAW020-2	P_{grac}::*seHas*:*tuaD*, Amp^R, ET for insertion of the HA biosynthetic operon into the *amyE* locus at *amyE*.P636T	Westbrook et al. (2016)
pAW003-4	$P_{grac.UPmod}$::*pgsA*:*clsA*, P_{araE}::*mazF*, *araR*, Spc^R, Erm^R, *B. subtilis* auto-evicting counter-selectable *thrC* integration vector	Westbrook, Ren, Moo-Young, et al. (2018)
pAW001-5	$P_{xylA,\ Bm}$::*comK*, *xylR*, P_{araE}::*mazF*, *araR*, Spc^R, Erm^R, *B. subtilis* counter-selectable *bpr* integration vector	This study
pAW002-5	$P_{xylA,\ Bm}$::*comK*:*comS*, *xylR*, P_{araE}::*mazF*, *araR*, Spc^R, Erm^R, *B. subtilis* counter-selectable *bpr* integration vector	This study
pAW003-5	$P_{xylA.SphI+1}$::P_{grac}::*ilvBHC*-gRNA, P_{araE}::*mazF*, *araR*, Spc^R, Erm^R, *B. subtilis* counter-selectable *thrC* integration vector	This study
pAW004-5	$P_{xylA.SphI+1}$::*bcd*-gRNA.P585T, $P_{xylA.SphI+1}$::P_{grac}::*ilvBHC*-gRNA, P_{araE}::*mazF*, *araR*, Spc^R, Erm^R, *B. subtilis* counter-selectable *thrC* integration vector	This study
pAW005-5	$P_{xylA.SphI+1}$::*leuA*-gRNA.P764NT, $P_{xylA.SphI+1}$::*bcd*-gRNA.P585T, $P_{xylA.SphI+1}$::P_{grac}::*ilvBHC*-gRNA, P_{araE}::*mazF*, *araR*, Spc^R, Erm^R, *B. subtilis* counter-selectable *thrC* integration vector	This study
pAW006-5	$P_{xylA.SphI+1}$::*amyE*-gRNA.P636T, P_{araE}::*mazF*, *araR*, Spc^R, Erm^R, *B. subtilis* counter-selectable *thrC* integration vector	This study
pAW007-5	$P_{xylA.SphI+1}$::*wprA*-gRNA.P1419T, $P_{xylA.SphI+1}$::*amyE*-gRNA.P636T, P_{araE}::*mazF*, *araR*, Spc^R, Erm^R, *B. subtilis* counter-selectable *thrC* integration vector	This study
pAW008-5	$P_{xylA.SphI+1}$::$P_{grac.UPmod}$::*alsSD*-gRNA, P_{araE}::*mazF*, *araR*, Spc^R, Erm^R, *B. subtilis* counter-selectable *thrC* integration vector	This study
pAW009-5	$P_{xylA.SphI+1}$::*ilvB*-gRNA.P1101NT, $P_{xylA.SphI+1}$::$P_{grac.UPmod}$::*alsSD*-gRNA, P_{araE}::*mazF*, *araR*, Spc^R, Erm^R, *B. subtilis* counter-selectable *thrC* integration vector	This study
pAW010-5	$P_{xylA.SphI+1}$::*ilvA*-gRNA.P581NT, $P_{xylA.SphI+1}$::*leuA*-gRNA.P764NT, $P_{xylA.SphI+1}$::*bcd*-gRNA.P585T, $P_{xylA.SphI+1}$::P_{grac}::*ilvBHC*-gRNA, P_{araE}::*mazF*, *araR*, Spc^R, Erm^R, *B. subtilis* counter-selectable *thrC* integration vector	This study
pAW011-5	$P_{xylA.SphI+1}$::$P_{grac.UPmod}$::*bcaP*-gRNA, P_{araE}::*mazF*, *araR*, Spc^R, Erm^R, *B. subtilis* counter-selectable *thrC* integration vector	This study
pAW012-5	$P_{xylA.SphI+1}$::*ilvH*-gRNA.P40T, P_{araE}::*mazF*, *araR*, Spc^R, Erm^R, *B. subtilis* counter-selectable *thrC* integration vector	This study
pAW013-5	$P_{xylA.SphI+1}$::*alsD*-gRNA.P99T, P_{araE}::*mazF*, *araR*, Spc^R, Erm^R, *B. subtilis* counter-selectable *thrC* integration vector	This study
pAW014-5	$P_{xylA.SphI+1}$::*pdhA*-gRNA.P116T, P_{araE}::*mazF*, *araR*, Spc^R, Erm^R, *B. subtilis* counter-selectable *thrC* integration vector	This study
pAW015-5	$P_{xylA.SphI+1}$::*sigF*-gRNA.P371T, P_{araE}::*mazF*, *araR*, Spc^R, Erm^R, *B. subtilis* counter-selectable *thrC* integration vector	This study
pAW016-5	P_{grac}::*ilvBHC* editing template, Amp^R	This study
pAW017-5	mut.*bcd*.P585T editing template, Amp^R	This study
pAW018-5	mut.*leuA*.P764NT editing template, Amp^R	This study
pAW019-5	P_{grac}::*ybgE*:*ywaA*, Amp^R, *B. subtilis amyE* integration vector	This study
pAW020-5	P_{grac}::*ilvD*, Amp^R, *B. subtilis wprA* integration vector	This study
pAW021-5	IlvH(N11A,G14D,N17F,N29H) editing template, Amp^R	This study
pAW022-5	$P_{grac.UPmod}$::*alsSD* editing template, Amp^R	This study
pAW023-5	P_{mtlA}::*alsSD* editing template, Amp^R	This study

(Continues)

TABLE 1 (Continued)

Strain or plasmid	Characteristics[a]	Source
pAW024-5	mut.*ilvB*.P1101NT editing template, Amp^R	This study
pAW025-5	mut.*ilvA*.P581NT editing template, Amp^R	This study
pAW026-5	mut.*alsD*.P99T editing template, Amp^R	This study
pAW027-5	$P_{grac.UPmod}$::*bcaP* editing template, Amp^R	This study
pAW028-5	mut.*sigF*.P371T editing template, Amp^R	This study
pAW029-5	mut.*pdhA*.P116T editing template, Amp^R	This study
pAW030-5	editing template to restore *thrC*, Amp^R	This study

Notes. [a]*alsD*: acetolactate decarboxylase; *alsS*: acetolactate synthase; *amyE*: α-amylase; *araR*: repressor of arabinose operons; *bcaP*: BCAA permease; *bcd*: BCAA dehydrogenase; *bpr*: bacillopeptidase F; *cas9*: CRISPR-associated protein 9 (Cas9; *Streptococcus pyogenes*); *comK*: master competence regulator; comS: competence protein S; *ilvA*: L-threonine dehydratase; *ilvB*: acetohydroxy-acid synthase catalytic subunit; *ilvC*: acetohydroxy-acid isomeroreductase; *ilvD*: dihydroxy-acid dehydratase; *ilvH*: native acetohydroxy-acid synthase regulatory subunit; *ilvH**: engineered acetohydroxy-acid synthase regulatory subunit; lacA: β-galactosidase; *leuA*: 2-isopropylmalate synthase; *mazF*: endoribonuclease (*Escherichia coli*); *pdhA*: E1α subunit of the pyruvate dehydrogenase complex; *sigF*: sporulation-specific transcription factor σ^F; *thrC*: threonine synthase; tracrRNA: trans-activating CRISPR RNA; *wprA*: cell wall-associated protease; *xylR*: xylose operon repressor (*Bacillus megaterium*); *ybgE*: BCAA aminotransferase; *ywaA*; BCAA aminotransferase; Neo^R: neomycin resistance cassette; Erm^R: erythromycin resistance cassette; Spc^R: spectinomycin resistance cassette; Amp^R: ampicillin resistance cassette.

results suggest that feedback inhibition of IlvBH by L-valine is not a critical issue, while acetate dissimilation may be limiting L-valine overproduction in Δ*pdhA B. subtilis* strains.

2 | MATERIALS AND METHODS

2.1 | Bacterial strains, primers, and plasmids

The *B. subtilis* strains used in this study are listed in Table 1. *E. coli* HI-Control™ 10G chemically competent cells (Lucigen, Middleton, WI) were prepared as electrocompetent cells as described previously (Sambrook & Russell, 2001) and used as host for plasmid construction. *B. subtilis* and *E. coli* strains were maintained as glycerol stocks at −80°C. Primers (Supporting Information Table S1) were synthesized by Integrated DNA Technologies (Coralville, IA). Plasmid pAX01 (ECE137) was obtained from the Bacillus Genetic Stock Center (Columbus, OH), and pgRNA-bacteria was a gift from Stanley Qi (Addgene, Cambridge, MA; plasmid, #44251).

2.2 | Plasmid and strain construction

DNA manipulation was performed using standard cloning techniques (Sambrook & Russell, 2001), and DNA sequencing was conducted by The Centre for Applied Genomics (TCAG, Ontario, Canada). Plasmid construction is described in detail in the Supporting Information. Strain construction is summarized in Table 2 in which the parent strain and donor plasmids corresponding to each new strain are identified.

2.3 | Competent cell preparation and transformation

Preparation and transformation of naturally competent *B. subtilis* was performed as previously described (Westbrook et al., 2016). To prepare artificially supercompetent strains, cells were plated on nonselective lysogeny broth (LB) agar containing (per L) 5 g of NaCl, 5 g of yeast extract, 10 g of tryptone, and 15 g of agar, and incubated overnight at 37°C. Prewarmed LB medium (20 ml) containing 5 mM of $MgSO_4$ was inoculated by cell patches from the overnight plate to

TABLE 2 Summary of parent strains and donor plasmids used for strain construction in this study

Parent strain	Donor plasmid(s)	Resulting strain
AW001-2	pAW002-5	AW001-5
AW001-5	pAW004-5, pAW016-5, pAW017-5	AW002-5
AW002-5	pAW006-5, pAW019-5	AW003-5
AW003-5	pAW007-5, pAW020-5	AW004-5
AW004-5	pAW012-5, pAW021-5	AW005-5
AW004-5	pAW009-5, pAW022-5, pAW024-5	AW006-5
AW005-5	pAW010-5, pAW018-5, pAW025-5	AW007-5
AW007-5	pAW008-5, pAW022-5	AW008-5
AW007-5	pAW008-5, pAW023-5	AW009-5
AW009-5	pAW013-5, pAW026-5	AW010-5
AW010-5	pAW011-5, pAW027-5	AW011-5
AW011-5	pAW014-5, pAW029-5	AW012-5
AW004-5	pAW014-5, pAW029-5	AW013-5
AW005-5	pAW014-5, pAW029-5	AW014-5
AW007-5	pAW014-5, pAW029-5	AW015-5
AW009-5	pAW014-5, pAW029-5	AW016-5
AW010-5	pAW014-5, pAW029-5	AW017-5
AW015-5	pAW015-5, pAW028-5	AW018-5
AW013-5	pAW010-5, pAW018-5, pAW025-5	AW019-5

OD_{600} 0.4–0.6, and the cultures were grown at 37°C and 280 revolutions per min (rpm). Once the cell density reached OD_{600} 0.8–1, xylose was added to the cultures at a final concentration of 10 g/L to induce the expression of *comK* and *comS*, and the induced cultures were incubated for 1.5 hr to develop the supercompetent state. 1.5 μg of gRNA delivery vector and 1.5 μg of each editing template were used per transformation, and transformed cells were incubated for 80 min at 280 rpm and 37°C, and plated on LB agar containing 12 g/L glucose (LBG) and 85 μg/mL of spectinomycin to select recombinants. All gRNA delivery vectors and editing templates were linearized with appropriate restriction enzymes before transformation. The same procedure was used to evict gRNA transcription cassettes from the *thrC* locus after each round of CRISPR-Cas9 genome editing, except that 1 μg of *Sca*I-linearized pAW030-5 was used per transformation, and cells were plated on LB agar containing 20 g/L arabinose (LBA) and subsequently tested for spectinomycin sensitivity (Westbrook et al., 2016). Media was supplemented with 3 g/L of sodium acetate when culturing Δ*pdhA* mutants.

2.4 | Cultivation medium and conditions

B. subtilis strains were plated on nonselective LB agar and grown overnight at 37°C. A single colony was used to inoculate 25 ml of nonselective LB, and the culture was grown for ~12 hr at 37°C and 280 rpm. The culture was then used to inoculate 20 ml of prewarmed nonselective cultivation medium (4% vol/vol) of the following composition (per L): Sucrose, 30 g; mannitol, 10 g; $(NH_4)_2SO_4$, 17 g; $K_2HPO_4{\cdot}3H_2O$, 18.3 g; KH_2PO_4, 6 g; trisodium citrate·$2H_2O$, 1 g; yeast extract, 5 g; leucine, 250 mg; isoleucine, 250 mg; $MgSO_4$,

FIGURE 2 Genome engineering strategies for L-valine overproduction in *B. subtilis*. Color legend for genes and promoters: Light blue, genes serving as integration sites; green, genes to be overexpressed from engineered promoters (dark blue); red, genes that are mutation targets (black segment indicates mutation); pink, native promoters and corresponding regulatory elements. Parent strains are identified in parentheses below the strain names. [a–e]: AW013-5, AW014-5, AW015-5, AW016-5, and AW017-5 are respective Δ*pdhA* derivatives of the corresponding strains. AW018-5 is a Δ*sigF* derivative of AW015-5, and AW019-5 is a Δ*leuA* Δ*ilvA* derivative of AW013-5. *alsD*: acetolactate decarboxylase; *alsS*: acetolactate synthase; *amyE*: α-amylase; *bcaP*: BCAA permease; *bcd*: BCAA dehydrogenase; *bpr*: bacillopeptidase F; *comK*: competence transcription factor; *comS*: competence protein S; *ilvA*: L-threonine dehydratase; *ilvB*: acetohydroxy-acid synthase catalytic subunit; *ilvC*: acetohydroxy-acid isomeroreductase; *ilvD*: dihydroxy-acid dehydratase; *ilvH*: native acetohydroxy-acid synthase regulatory subunit; *ilvH**: engineered acetohydroxy-acid synthase regulatory subunit; *leuA*: 2-isopropylmalate synthase; *pdhA*: E1α subunit of the pyruvate dehydrogenase complex; *sigF*: sporulation-specific transcription factor σ^F; *wprA*: cell wall-associated protease; *ybgE*: BCAA aminotransferase; *ywaA*; BCAA aminotransferase; $P_{ilv\text{-}leu}$: *ilvBHC-leuABCD* promoter and corresponding regulatory elements; P_{als}: *alsSD* promoter and corresponding regulatory elements; P_{bcaP}: *bcaP* promoter and corresponding regulatory elements; $P_{xylA,Bm}$: xylose-inducible *xylA* promoter (*Bacillus megaterium*); P_{grac}: constitutive promoter; P_{mtlA}: mannitol-inducible *mtlA* promoter; $P_{grac.UPmod}$: constitutive promoter [Color figure can be viewed at wileyonlinelibrary.com]

120 mg; $CaCl_2$, 5.5 mg; $FeCl_2{\cdot}6H_2O$, 13.5 mg; $MnCl_2{\cdot}4H_2O$, 1 mg; $ZnCl_2$, 1.7 mg; $CuCl_2{\cdot}2H_2O$, 0.43 mg; $CoCl_2{\cdot}6H_2O$, 0.6 mg; $Na_2MoO_4{\cdot}2H_2O$, 0.6 mg. Cultures were grown at 37°C and 280 rpm, and the medium was supplemented with 3 g/L of sodium acetate when culturing Δ*pdhA* mutants. To assess cell growth in the presence of excess L-valine, cells were grown in a minimal medium of the following composition (per L): sucrose, 10 g; $(NH_4)_2SO_4$, 12 g; $K_2HPO_4{\cdot}3H_2O$, 18.3 g; KH_2PO_4, 6 g; trisodium citrate·$2H_2O$, 1 g; $MgSO_4$, 120 mg; $CaCl_2$, 5.5 mg; $FeCl_2{\cdot}6H_2O$, 13.5 mg; $MnCl_2{\cdot}4H_2O$, 1 mg; $ZnCl_2$, 1.7 mg; $CuCl_2{\cdot}2H_2O$, 0.43 mg; $CoCl_2{\cdot}6H_2O$, 0.6 mg; $Na_2MoO_4{\cdot}2H_2O$, 0.6 mg. L-Valine was supplemented at a concentration of 3, 8, or 20 g/L as indicated.

2.5 | L-Valine quantification

L-Valine was first converted to its α-hydroxy acid, that is, 2-hydroxy-3-methylbutyric acid, via nitrosation before quantification via high-performance liquid chromatography (HPLC) as previously described (Ulusoy, Ulusoy, Pleissner, & Eriksen, 2016) with minor modifications. Culture samples were centrifuged at 13,000 rpm for 10 min, and the cell-free supernatant was diluted as required. 500 µl of cell-free supernatant was mixed with 100 µl of 1 M KNO_2, and the nitrosation reaction was initiated by adding 20 µl of 3 M HCl. The reaction was conducted at 45°C for 40 min and was stopped by adding 100 µl of 2 M NaOH. The nitrosated samples were then degassed in an ultrasonic water bath at 50°C for 30 min, and filter-sterilized before HPLC analysis. The HPLC system consists of a Shimadzu (Kyoto, Japan) LC-10AT solvent delivery unit, Shimadzu RID-10A refractive index detector, Shimadzu CTO-20A column oven, and an Aminex HPX-87H chromatographic column (Bio-Rad Laboratories, Hercules, CA). The column and detector temperatures were maintained at 27 and 30°C, respectively, and the flow rate of the mobile phase (i.e., 5 mM of H_2SO_4) was 0.4 ml/min. Signal acquisition and data processing were performed with Clarity Lite (DataApex, Prague, Czech Republic).

3 | RESULTS

3.1 | Relief of feedback inhibition for L-valine overproduction in *B. subtilis*

To derive L-valine-overproducing strains of *B. subtilis*, we used our recently developed CRISPR-Cas9 toolkit (Westbrook et al., 2016) to manipulate various key genes (Figure 2). Overexpression of *comK*, encoding the competence transcription factor ComK, and *comS*, encoding competence protein S (ComS), during exponential growth can significantly improve the transformation efficiency of *B. subtilis* strains, compared to transformation via natural competence (Rahmer, Heravi, & Altenbuchner, 2015). Accordingly, we constructed the supercompetent strain AW001-5 that coexpressed xylose-inducible *comK* and *comS* from the *bpr* locus (Figure 2). Given that *ilvBHC* are expressed as part of a single operon and the regulatory elements controlling its expression are spatially defined, we chose to replace the 677 bp region upstream of the *ilvB* ribosome binding site (including a TnrA box [Tojo et al., 2004], all four CodY binding sites, a catabolite repression element and its upstream binding site [Fujita, Satomura, Tojo, & Hirooka, 2014], the $tRNA^{Leu}$ T-box, and $P_{ilv\text{-}leu}$) with the strong constitutive promoter P_{grac} (Phan, Nguyen, & Schumann, 2012) in strain AW002-5 (Figure 2). In addition, we simultaneously mutated *bcd* to prevent the conversion of L-valine to 2-ketoisovalerate in AW002-5. Due to the repression of *ybgE* and *ywaA* expression by CodY via its interaction with one or more binding sites upstream of each respective gene (Belitsky & Sonenshein, 2013), we chose to overexpress both genes as a single operon to enhance L-valine overproduction in strain AW003-5, in which a P_{grac}::*ybgE*::*ywaA* expression cassette was integrated at the *amyE* locus (Figure 2). Similarly, the expression of *ilvD* is repressed by CodY via an upstream binding site, prompting us to overexpress *ilvD* in strain AW004-5, in which a P_{grac}::*ilvD* expression cassette was integrated at the *wprA* locus (Figure 2).

The inhibition of AHAS by BCAAs has been well documented (Chipman et al., 1998; Mendel et al., 2001). IlvH of *B. subtilis* is a reportedly L-valine-sensitive AHAS that is similar in structure to AHAS III of *E. coli* (i.e., $IlvH^{Ec}$), and both enzymes possess several conserved amino acid residues potentially associated with L-valine sensitivity (Kaplun et al., 2006; Livshits et al., 2004; Mendel et al., 2001). Based on the identified L-valine-sensitive amino acids in $IlvH^{Ec}$, we introduced three point mutations to conserved amino acid residues in *B. subtilis* IlvH, that is, N11A, G14D, and N29H. A fourth point mutation, that is, N17F, was also introduced as the point mutation S17F reduced the L-valine sensitivity of $IlvH^{Ec}$ (Livshits et al., 2004), and N and S are both polar amino acids. The specified point mutations were introduced into native *B. subtilis* IlvH in strain AW005-5, which expressed engineered IlvH, that is, IlvH* (Figure 2). As AlsS is a dedicated ALS rather than an AHAS, as is the case for IlvBH, it can facilitate L-valine but not L-isoleucine biosynthesis. This moved us to investigate the performance of strains expressing AlsS in the absence of functional IlvBH for L-valine overproduction, by attempting to construct an editing template for the genomic integration of a P_{grac}::*ilvD*:*alsS* expression cassette at the *wprA* locus of AW003-5, in parallel with the mutation of *ilvB*. However, this plasmid was not stable in *E. coli* due to the presence of *alsS*, prompting us to replace the 186 bp region between bp 29 of the *alsR* open reading frame (ORF) and bp 2 of the *alsS* ORF, including promoters P_{alsR} and P_{alsSD}, and the AlsR regulatory and activator binding sites (Frädrich et al., 2012), with the relatively strong constitutive promoter $P_{grac.UPmod}$ (Westbrook, Ren, Moo-Young, & Chou, 2018) in strain AW006-5, in which we simultaneously mutated *ilvB* (Figure 2).

AW001-5 (i.e., the control strain), AW002-5, AW003-5, AW004-5, AW005-5, and AW006-5 were evaluated for L-valine overproduction in shake flask cultures. The cell density reached OD_{600} 13.3 after 24 hr (Figure 3a) and the L-valine titer was below the detectable limit of ~0.1 g/L in cultures of AW001-5 (Figure 3b). Cell growth was nearly identical between cultures of AW002-5 and AW001-5 (Figure 3a), while L-valine was detectable after 12 hr with the titer reaching 1.2 g/L after 24 hr (Figure 3b), representing a >12-fold

increase in L-valine production compared to AW001-5. On the other hand, cell growth was delayed in cultures of AW003-5, compared to AW002-5 (Figure 3a), and L-valine was detectable after 8 hr with the titer reaching 1.48 g/L after 24 hr (Figure 3b). The culture performance was markedly different for AW004-5 as the maximum cell density of OD_{600} 8.1 was attained after 12 hr, compared to OD_{600} 12.7 after 24 hr for AW003-5 (Figure 3a), and L-valine was detectable after 4 hr with the titer reaching 1.33 g/L after 12 hr without further increasing. Similarly, the cell density peaked at OD_{600} 7.7 after 12 hr in cultures of AW005-5 (Figure 3a), and L-valine was detectable after 4 hr with the titer reaching 1.44 g/L after 24 hr (Figure 3b). The significantly improved L-valine production in cultures of AW002-5, compared to AW001-5, indicates that the expression of *ilvBHC* from $P_{ilv\text{-}leu}$ was tightly repressed in our cultivation medium, presumably due to the presence of exogenous amino acids as previously described. The delay in L-valine overproduction in cultures of AW002-5 suggests potential repression of the expression of native *ybgE*, *ywaA*, and *ilvD* by the activity of CodY, which gradually diminishes as the cultures progress and the amino acids are depleted. This hypothesis is supported by the observation that the delay in L-valine overproduction was respectively reduced by 4 and 8 hr in cultures of AW003-5 (which overexpresses *ybgE* and *ywaA*) and AW004-5 (which overexpresses *ybgE*, *ywaA*, and *ilvD*). In addition, the dramatic increase in the L-valine production rate between 8 and 12 hr in cultures of AW003-5, compared to AW002-5 (Table 3), may indicate that the conversion of 2-ketoisovalerate to L-valine by YbgE or YwaA limits the rate of L-valine production in *B. subtilis*, which has also been proposed in *C. glutamicum* (Oldiges et al., 2014). However, the similar final L-valine titers in cultures of AW002-5, AW003-5, and AW004-5 suggests that L-valine overproduction was not limited by the expression of *ybgE*, *ywaA*, or *ilvD* after CodY activity decreased. Moreover, as the maximum cell density was lower (Figure 3a) and L-valine overproduction was not drastically improved (Figure 3b) in cultures of AW004-5, compared to AW003-5, we speculate that the overexpression of IlvD was somewhat deleterious to cell physiology and/or the early overproduction of L-valine reduced the availability of resources for biomass accumulation. In addition, the similar culture performance observed between AW004-5 and AW005-5 suggests that L-valine feedback inhibition of native IlvBH in *B. subtilis* was modest at this level of L-valine overproduction. Lastly, the cell density was markedly higher (OD_{600} 12.3; Figure 3a) and the L-valine titer was comparable (1.5 g/L; Figure 3b) after 24 hr in cultures of AW006-5, compared to AW005-5, although cell growth and L-valine overproduction were severely delayed, suggesting that expressing AlsS in place of IlvBH* was not advantageous for L-valine overproduction.

3.2 | Manipulation of key genes associated with L-valine overproduction in *B. subtilis*

We next sought to identify potential bottlenecks limiting L-valine overproduction in *B. subtilis* to improve culture performance. L-Leucine and L-valine biosynthesis are in direct competition for the intermediate 2-ketoisovalerate (Figure 1), while L-isoleucine is also derived from pyruvate by the same enzymes that synthesize L-valine (i.e., IlvBHCD, YbgE, and YwaA; Figure 1). Accordingly, we simultaneously mutated *leuA* and *ilvA* in strain AW007-5 (Figure 2). The cell density peaked at OD_{600} 7.5 after 12 hr (Figure 4a) and the L-valine titer reached 1.5 g/L (Figure 4b) in cultures of AW007-5, representing a marginal improvement in L-valine overproduction relative to AW005-5 (Figure 3b), suggesting that L-valine overproduction was not affected by the two side pathways under this genetic background. To determine if L-valine overproduction may be limited by 2-acetolactate levels in AW007-5, we inserted $P_{grac.UPmod}$ in place of P_{alsSD} in strain AW008-5. However, a severe growth defect was observed for AW008-5, prompting us to insert a weaker inducible promoter in place of P_{alsSD}, that is, the mannitol-inducible promoter P_{mtlA} (Heravi, Wenzel, & Altenbuchner, 2011), in strain AW009-5 (Figure 2). The peak cell density and final L-valine titer decreased to OD_{600} 3.6 after 8 hr (Figure 4a) and 1.27 g/L (Figure 4b), respectively, in cultures of AW009-5. We postulated that the enhanced conversion of 2-acetolactate to acetoin due to the increased expression of *alsD* may have hindered the culture performance of AW009-5 and, thus, mutated *alsD* in strain AW010-5 (Figure 2). However, the peak cell density and final L-valine titer marginally increased to OD_{600} 4 after 24 hr (Figure 4a), and 1.35 g/L (Figure 4b), respectively, in cultures of AW010-5, suggesting that 2-acetolactate availability was not limiting L-valine overproduction in our strains.

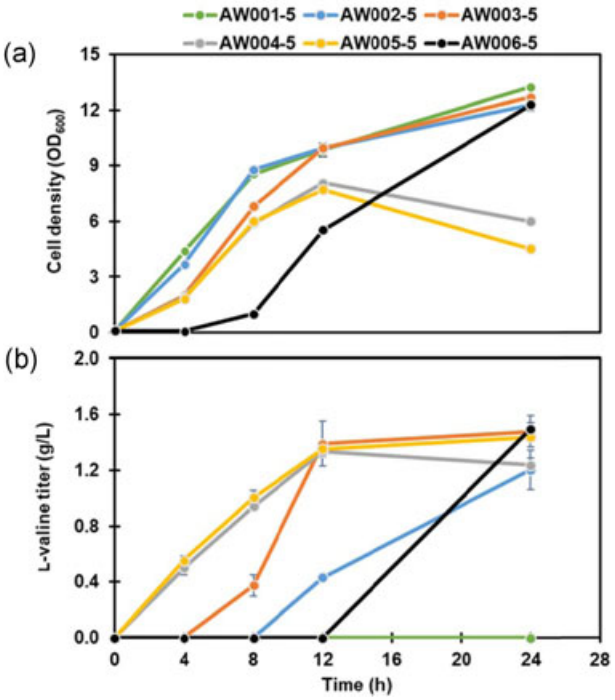

FIGURE 3 Time profiles of (a) cell density and (b) L-valine titer in cultures of AW001-5, AW002-5, AW003-5, AW004-5, AW005-5, and AW006-5. *SD* of experiments performed in duplicate are shown in (a) and (b). ND indicates that the L-valine titer was below the detectable limit of ~0.1 g/L. SD: standard deviation [Color figure can be viewed at wileyonlinelibrary.com]

TABLE 3 L-Valine production rates in cultures from this study

	L-Valine production rate ($g \cdot L^{-1} \cdot h^{-1}$)			
Strain	0–4 hr	4–8 hr	8–12 hr	12–24 hr
AW002-5	0	0	0.108	0.032
AW003-5	0	0.094	0.254	0.007
AW004-5	0.125	0.110	0.099	−0.008
AW005-5	0.139	0.112	0.088	0.007
AW006-5	0	0	0	0.125
AW007-5	0.145	0.144	0.070	0.005
AW009-5	0.128	0.133	0.072	−0.005
AW010-5	0.158	0.133	0.033	0.005
AW011-5	0.148	0.102	0.074	−0.005
AW012-5	0.092	0.188	0.128	0.019
AW013-5	0.104	0.149	0.040	0.086
AW014-5	0.102	0.155	0.119	0.075
AW015-5	0.093	0.228	0.331	0.167
AW016-5	0.100	0.236	0.260	0.052
AW017-5	0.103	0.195	0.117	0.039
AW018-5	0.116	0.326	0.256	0.152
AW019-5	0.080	0.381	0.205	0.078

L-Valine overproduction was enhanced by overexpressing the BCAA exporters YgaZH in *E. coli* (Park et al., 2007) and BrnFE in *C. glutamicum* (Chen et al., 2015). Accordingly, we manipulated the expression of *bcaP*, encoding a key L-valine-associated permease in *B. subtilis*, by replacing the 214 bp region upstream of the *bcaP* start codon, including CodY-I, CodY-II, and P_{bcaP}, with $P_{grac.UPmod}$ in strain AW011-5 (Figure 2). The peak cell density (OD_{600} 3.5 after 8 hr) and final L-valine titer (1.24 g/L) declined slightly in cultures of AW011-5 (Figure 4a,b), compared to AW010-5, suggesting that L-valine secretion was not limiting overproduction in our strains. The modest reduction in cell growth and L-valine overproduction may have resulted from the deleterious physiological effects of the overexpression of transmembrane transporter proteins, which we have previously observed in *B. subtilis* strains engineered for enhanced hyaluronic acid production (Westbrook, Ren, Oh, Moo-Young, & Chou, 2018).

Finally, we attempted to increase pyruvate levels by mutating *pdhA* in strain AW012-5 (Figure 2). The peak cell density and final L-valine titer increased by 60% (OD_{600} 5.6 after 12 hr) and 50% (1.86 g/L) in cultures of AW012-5 (Figure 4a,b), compared to AW011-5. These results suggest that pyruvate availability limits L-valine overproduction in *B. subtilis*, and such limitation was also identified in L-valine-overproducing strains of *C. glutamicum* (Oldiges et al., 2014).

3.3 | Inactivating the L-leucine and L-isoleucine pathways under the ΔpdhA background

Upon identifying pyruvate availability as the major bottleneck limiting L-valine overproduction in *B. subtilis*, we reexamined previous strain engineering strategies in the Δ*pdhA* background by constructing strains AW013-5, AW014-5, AW015-5, AW016-5, and AW017-5 (Figure 2). As expected, the mutation of *pdhA* resulted in significant improvements to the L-valine titer (Figures 4 and 5b) and production rates (Table 3) in all previously derived strains. The final L-valine titers in cultures of AW013-5 (2.2 g/L; Figure 5b) and AW014-5 (2.4 g/L; Figure 5b), that is, respective Δ*pdhA* mutants that express native *ilvH* and *ilvH** were similar, further suggesting that L-valine feedback inhibition of IlvBH is minimal in *B. subtilis*. Notably, the L-valine titer reached 4.61 g/L in cultures of AW015-5 (Figure 5b), representing a 92% increase compared to AW014-5. These observations suggest that a competition for cellular resources exists between the pathways for BCAA biosynthesis, such that *leuA* and *ilvA* are critical targets for mutation to enhance L-valine overproduction in *B. subtilis* in spite of the resulting auxotrophy. On other hand, the L-valine titer declined to 3.01 g/L in cultures of AW016-5 (Figure 5b), suggesting, once again, that upregulating the expression of *alsS* in parallel with *ilvBH** impedes L-valine biosynthesis. In contrast to the *alsD* mutant AW010-5 that produced a similar L-valine titer to its parent strain AW009-5, AW017-5 produced even less L-valine than AW016-5 (i.e., 2.14 g/L compared with 3.01 g/L; Figure 5b), indicating that *alsD* is not an appropriate target for mutation. Sporogenesis occurs in *B. subtilis* cultures in response to nutrient depletion and high cell densities (Errington, 2003), potentially hampering culture performance and preventing its industrial application (Zhang, Duan, & Wu, 2016). Hence, we also selected *sigF*, encoding transcription factor σ^F that controls the expression of genes that initiate prespore development (Errington, 2003), as a mutation target in strain AW018-5. While the cell density profiles (Figure 6a) and L-valine titers (Figure 6b) were similar in cultures of AW015-5 and AW018-5, the absence of sporulation is a desirable trait for industrial production strains.

3.4 | Feedback inhibition of IlvBH is minimal in *B. subtilis*

Given the similar final L-valine titers in cultures of AW013-5 and AW014-5 (i.e., 2.2 g/L compared to 2.4 g/L; Figure 5b), which are respective Δ*pdhA* mutants that express native *ilvH* and *ilvH**, we suspected that L-valine feedback inhibition of IlvBH may not be a critical issue in *B. subtilis*. To gain further insight into this matter, we simultaneously mutated *leuA* and *ilvA* in strain AW019-5. The peak cell density and final L-valine titer reached OD_{600} 8 after 24 hr (Figure 6a) and 3.6 g/L (Figure 6b), respectively, in cultures of AW019-5, representing no significant difference in cell growth and a 22% decrease in the L-valine titer compared to cultures of AW015-5 (4.61 g/L; Figure 6b), that is, a strain expressing *ilvH** that is otherwise identical. We also performed growth experiments with AW004-5 and AW005-5 in a minimal medium containing various concentrations of L-valine to establish if growth inhibition occurred in the presence of excess L-valine. The growth profiles were nearly identical in cultures of AW004-5 and AW005-5 for L-valine concentrations up to 20 g/L (Figure 7), indicating that feedback inhibition of IlvBH by L-valine is not significant enough to affect cell growth. In fact, the respective final cell densities increased by 37% and 43% in cultures of

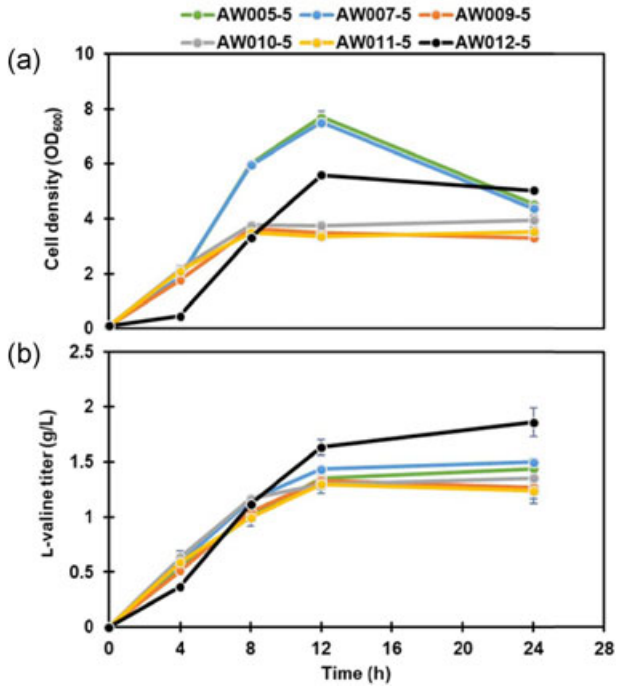

FIGURE 4 Time profiles of (a) cell density and (b) L-valine titer in cultures of AW005-5, AW007-5, AW009-5, AW010-5, AW011-5, and AW012-5. *SD* of experiments performed in duplicate are shown in (a) and (b). SD: standard deviation [Color figure can be viewed at wileyonlinelibrary.com]

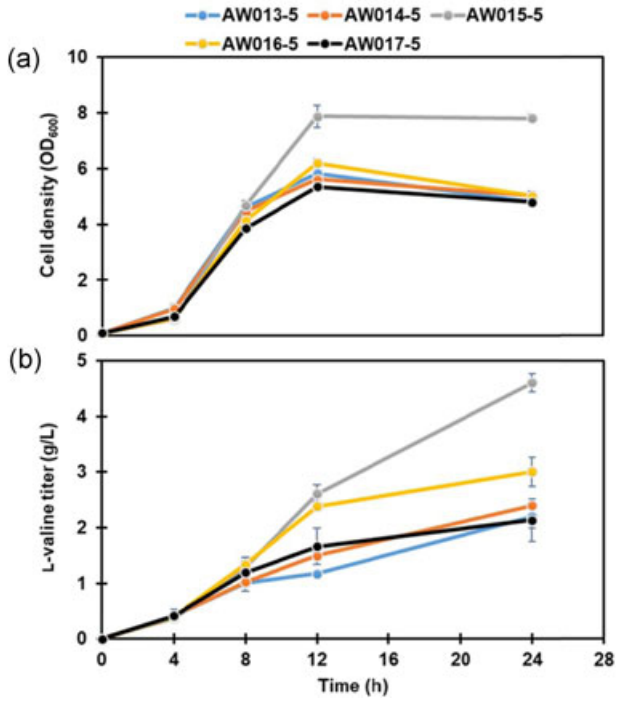

FIGURE 5 Time profiles of (a) cell density and (b) L-valine titer in cultures of AW013-5, AW014-5, AW015-5, AW016-5, and AW017-5. *SD* of experiments performed in duplicate are shown in (a) and (b). SD: standard deviation [Color figure can be viewed at wileyonlinelibrary.com]

AW004-5 and AW005-5 containing 20 g/L of L-valine, compared to the respective controls without supplemental L-valine, suggesting that YbgE and/or YwaA could convert L-valine to 2-ketoisovalerate to initiate L-valine catabolism.

4 | DISCUSSION

Due to its well-characterized genetic profile and ease of genetic manipulation, robust growth characteristics in simple media, and proven track record as a GRAS biomanufacturing platform, *B. subtilis* is a logical choice as a production host for amino acids. Here, we have demonstrated high-level L-valine overproduction in engineered *B. subtilis* as a first step toward its development into an industrially relevant production host for amino acids. Importantly, our engineered *B. subtilis* strains contain no replicating plasmids and, therefore, do not require antibiotic selection and are inherently more stable than previously developed L-valine-overproducing strains of *E. coli* and *C. glutamicum*.

The feedback inhibition of bacterial AHAS is a conserved feature among many, but not all, such enzymes (Chipman et al., 1998). Presumably due to the presence of the regulatory subunit (i.e., IlvH) that bears similarity to L-valine-sensitive $IlvH^{Ec}$, IlvBH from *B. subtilis* has been identified as a L-valine-sensitive homologue of AHAS III from *E. coli* (Mendel et al., 2001). The half maximal inhibitory concentration (IC_{50}) of L-valine for the IlvBH homologue of *C. glutamicum*, that is, $IlvBN^{Cg}$, is as low as 105 mg/L (Leyval, Uy, Delaunay, Goergen, & Engasser, 2003), and the minimum inhibitory

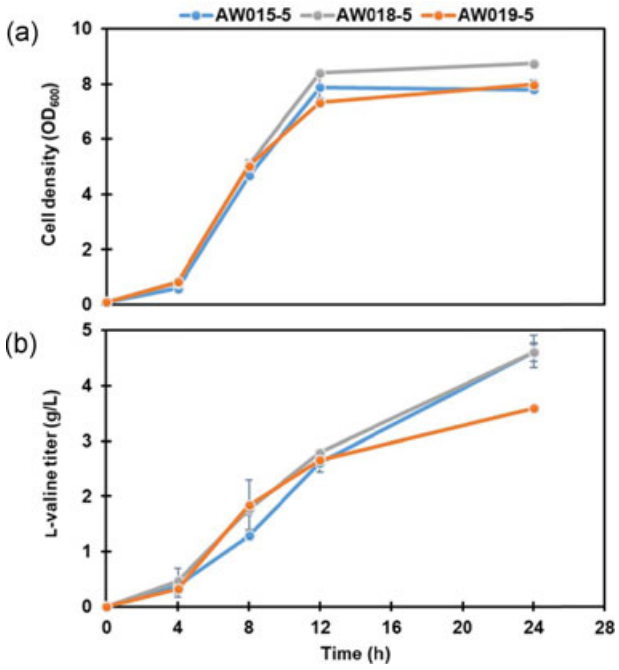

FIGURE 6 Time profiles of (a) cell density and (b) L-valine titer in cultures of AW015-5, AW018-5, and AW019-5. *SD* of experiments performed in duplicate are shown in (a) and (b). SD: standard deviation [Color figure can be viewed at wileyonlinelibrary.com]

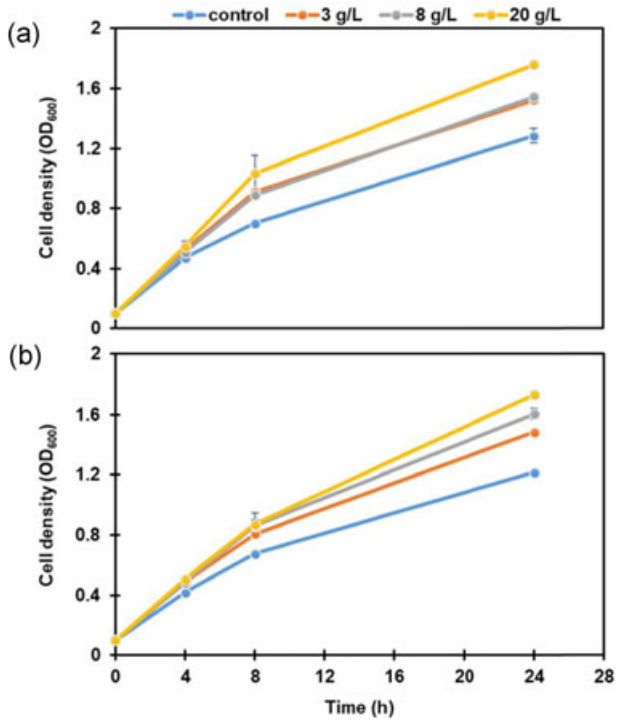

FIGURE 7 Time profiles of the cell density in cultures of (a) AW004-5 and (b) AW005-5 containing no supplemental L-valine (control), or 3, 8, or 20 g/L of L-valine. *SD* of experiments performed in duplicate are shown in (a) and (b). SD: standard deviation [Color figure can be viewed at wileyonlinelibrary.com]

concentration of L-valine in *E. coli* K-12 and its derivatives, which lack functional L-valine-insensitive AHAS II, is as low as 2 mg/L (Kutukova et al., 2005). On other hand, *B. subtilis* 168 can grow in a medium containing at least 2.3 g/L of L-valine as the sole nitrogen source (Debarbouille et al., 1999), indicating that IlvBH is significantly less sensitive to L-valine compared to $IlvBH^{Ec}$. Our results are in agreement with this observation, as the L-valine titer reached 3.6 g/L in cultures of AW019-5, and cell growth was not significantly different between cultures of AW015-5 and AW019-5. We also observed that AW004-5 and AW005-5, that is, strains expressing native *ilvH* and $ilvH^{*}$, exhibited similar growth profiles in a minimal medium containing excess L-valine, with an ~40% increase in the final cell density obtained in cultures of both strains containing 20 g/L of L-valine, compared to the controls without supplemental L-valine (Figure 7). This is in contrast to the prior observation that a Δ*bcd* mutant of *B. subtilis* could not grow in a minimal medium containing L-valine as the sole nitrogen source (Debarbouille et al., 1999). However, the expression of native *ybgE* and *ywaA* were presumably repressed by L-valine-activated CodY in the cited study. The improved L-valine overproduction in cultures of AW015-5, compared to AW019-5, may result from a mild degree of feedback inhibition of IlvBH that is not sufficient to repress growth. Moreover, the L-valine production rate was 67% higher in cultures of AW019-5, compared to AW015-5, between 4 and 8 hr, although was significantly lower during the remainder of the cultivation (Table 3), further suggesting partial feedback inhibition of IlvBH as the L-valine titer increased. Another possibility is that $IlvH^{*}$ modulated the activity of the $IlvBH^{*}$ holoenzyme, resulting in increased flux through the L-valine biosynthetic pathway. However, further investigation is required to establish the cause of the modest improvements to culture performance in strains expressing $ilvH^{*}$.

Given that AlsS is a dedicated ALS, one might expect its overexpression to be beneficial to L-valine overproduction, compared to IlvBH which catalyzes two reactions (i.e., from pyruvate to 2-acetolactate during L-valine biosynthesis, and from pyruvate and 2-ketobutyrate to 2-aceto-2-hydroxybutyrate during L-isoleucine biosynthesis). Interestingly, upregulating the expression of the *alsSD* operon in the Δ*ilvB* background in AW006-5 resulted in a severe delay in cell growth and L-valine overproduction in our production medium, while the overnight growth of AW006-5 in LB-based seed culture was poor compared to all other strains evaluated in this study (data not shown). Note that the activity of dedicated ALS from acetoin-producing bacteria is optimal under low pH (~pH 6; Chipman et al., 1998), and that the expression of *alsSD* is induced in the presence of acetate and a low pH in *B. subtilis* (Frädrich et al., 2012). Cell growth and L-valine overproduction are initially poor in our production medium that contains excess sucrose. Then, acetate potentially accumulates with a concomitant decrease in the pH of the culture, inducing the activity of AlsS. On the other hand, cell growth, and presumably L-valine overproduction, remain low in LB medium, which lacks a dedicated carbon source for culture acidification. The compromised culture performance of AW017-5, that is, a strain in which the expression of *alsS* was upregulated and *alsD* was mutated, compared to AW016-5 in which *alsD* was intact, suggests that 2-acetolactate levels are sufficient and do not limit the overall L-valine biosynthesis in our engineered strains. Note that acetoin produced during carbon overflow metabolism in strains with intact *alsD* may serve as a carbon source in the later stages of the culture when sucrose is depleted (Renna et al., 1993), such that acetoin secretion may have contributed to the improved culture performance of AW016-5, compared to AW017-5. Furthermore, upregulating the expression of AlsS in AW009-5 resulted in a 52% decrease in the maximum cell density without an improvement to the L-valine titer, compared to cultures of AW007-5 (Figure 4). We speculate that this negative physiological response of *B. subtilis* to the expression of AlsS in the presence of functional IlvBH resulted from depleted levels of the key metabolite pyruvate. This is supported by the observation that the maximum cell density obtained in cultures of AW006-5 (i.e., a strain constitutively expressing AlsS without functional IlvBH) was similar to that of the parent strain AW001-5 (Figure 3a). Moreover, the maximum cell density in cultures of AW016-5 (a Δ*pdhA* derivative of AW009-5) declined by only 21%, compared to AW015-5 (a Δ*pdhA* derivative of AW007-5), indicating that increased pyruvate availability due to the mutation of *pdhA* could partially compensate for the pyruvate consumed by AlsS in the functional IlvBH background in AW016-5. Note that the L-valine production rates were similar between cultures of AW015-5 and AW016-5 until 8 hr, after which the L-valine production rate of AW015-5 was significantly higher for the remainder of the cultivation (Table 3). This

may be attributed to a pyruvate deficiency in AW016-5 upon entering the stationary phase due to the increased expression of *pycA*, encoding pyruvate carboxylase (PycA), which is cotranscribed with *ftsW* at a high level at the end of exponential phase (Lu et al., 2007; Sierro, Makita, de Hoon, & Nakai, 2007).

BCAA exporters have been overexpressed in *E. coli*, that is, YgaZH (Park et al., 2007), and *C. glutamicum*, that is, BrnFE (Chen et al., 2015), and their overexpression significantly improved L-valine production in both hosts. Of the four aforementioned proteins analyzed via BLAST (Johnson et al., 2008), only BrnF shared significant similarity to a certain *B. subtilis* protein. Specifically, BrnF and AzlC, a component of the 4-azaleucine transporter AzlCD (encoded by *azlCD*) from *B. subtilis* (Belitsky, 2015), are 31% identical (76% coverage; score 83.6). However, mutation of *azlCD* did not significantly affect the expression of CodY-regulated genes in the presence of BCAAs, suggesting that it does not play a significant role in the regulation of cellular L-valine levels (Belitsky, 2015). On the other hand, *bcaP* is among the highly CodY-regulated genes in *B. subtilis*, and CodY activity is modulated in a negative feedback loop by the expression of *bcaP* in a minimal medium containing only BCAAs (Belitsky, 2015). Though BcaP is the most efficient permease for the uptake of L-valine, our attempts of promoter engineering to enhance *bcaP* expression did not improve L-valine overproduction. It appears that the secretion of L-valine is naturally efficient in *B. subtilis* to service the production capacity of our engineered strains. However, CodY should be highly active in L-valine overproducing strains, such that *bcaP* expression from its native promoter should be downregulated. Accordingly, the facilitated export of L-valine could be mediated by a currently unidentified exporter(s) of BCAAs other than BcaP. Alternatively, based on the hydrophobicity of L-valine and its relatively high lipid/water phase partition coefficient, it is plausible that L-valine can passively diffuse across the cell membrane at significant rates (Krämer, 1994). Further investigation is required to clarify the dominant mechanism by which excess L-valine is secreted in *B. subtilis*, such that enhanced L-valine overproduction may be achieved by overexpressing a dedicated BCAA exporter, or through engineering or chemical treatment of the cell membrane to enhance permeability.

Importantly, our results show that pyruvate availability is limiting L-valine overproduction in *B. subtilis*. Such limited pyruvate pool also occurred in *C. glutamicum* (Oldiges et al., 2014), but not *E. coli* (Park, Kim, et al., 2011; Park et al., 2007), upon L-valine overproduction. The pyruvate limitation in *B. subtilis* is not surprising as its metabolism is suboptimal in the presence of preferred carbon sources due to regulatory mechanisms designed to carefully control metabolic fluxes at the expense of biomass accumulation, enabling a rapid response to environmental changes (Fischer & Sauer, 2005). In our recent study, to circumvent the rigid flux distribution at the glucose-6-P and fructose-6-P nodes, where glycolysis, the pentose phosphate pathway, and cell wall biosynthesis diverge, we successfully applied CRISPR interference (CRISPRi) to reduce the expression of enzymes at the branch points of these central metabolic pathways, in turn, significantly enhancing heterologous hyaluronic acid production in *B. subtilis* (Westbrook, Ren, Oh, et al., 2018). This approach may also prove effective in diverting additional pyruvate or 2-ketoisovalerate from competing metabolic pathways toward L-valine overproduction. For example, we were unsuccessful in mutating *panB*, encoding ketopantoate hydroxymethyltransferase (PanB) which converts 2-ketosiovalerate to 2-dehydropantoate during pantothenate biosynthesis, in our engineered strains, such that it may be an appropriate target for transcriptional repression to improve L-valine overproduction. However, we have observed that even subtle differences in the repression efficiency of target gene expression can significantly alter cell growth and culture performance, and that the repression efficiency afforded by dCas9-targeting gRNAs is difficult to anticipate, such that several gRNAs should be designed for a single target to obtain the full benefits of its repression (Westbrook, Ren, Moo-Young, et al., 2018; Westbrook, Ren, Oh, et al., 2018). One potentially beneficial aspect of the *B. subtilis* metabolism for L-valine overproduction is the general excess of intracellular NADPH that exists due to strict flux partitioning at the glucose-6-P node (Fischer & Sauer, 2005; Zamboni et al., 2005). As the biosynthesis of 1 mol of L-valine requires 2 mol of NADPH (Figure 1), the natural overabundance of NADPH is potentially a major advantage during L-valine overproduction. Finally, the substantial increase in the L-valine titer in cultures of AW015-5, compared to AW014-5 (Figure 5b), due to the simultaneous mutation of *leuA* and *ilvA* under the Δ*phdA* background is a similar phenomenon to that observed upon the mutation of *alaT*, encoding an aminotransferase that converts pyruvate and L-glutamate to L-alanine and 2-ketoglutarate (AlaT), and *ilvA* in *C. glutamicum* (Chen et al., 2015). In our study, mutating *leuA* is essential as *ilvBHC* and *leuABCD* comprise a single operon, such that significant L-leucine production is inevitable in strains in which $P_{ilv\text{-}leu}$ has been replaced to relieve transcriptional regulation. On the other hand, while the expression of *ilvA* is likely repressed by CodY (Molle et al., 2003) under our cultivation conditions, abolishing L-isoleucine biosynthesis via *ilvA* mutation could block such flux divergence even when CodY is inactive.

The titers obtained in shake flask cultivations of AW015-5 and AW018-5 are lower than those reported for *E. coli* and *C. glutamicum* engineered for L-valine overproduction (Supporting Information Table S2). While direct comparisons of experimental results obtained under significantly different conditions may not be entirely meaningful, our experiences with batch and fed-batch cultivations indicate that acetate dissimilation is limiting L-valine overproduction in AW018-5 (data not shown). The slow rate of acetate dissimilation can be attributed to the absence of a glyoxylate shunt in *B. subtilis* (Kabisch et al., 2013), which is present in both *E. coli* (Maloy & Nunn, 1982) and *C. glutamicum* (Bott & Eikmanns, 2013). However, acetate metabolism was markedly improved in *B. subtilis* via the expression of isocitrate lyase and malate synthase from *Bacillus licheniformis*, effectively completing the glyoxylate shunt in *B. subtilis* (Kabisch et al., 2013). Moreover, strategies such as promoter engineering to modulate the expression of *aceE*, encoding the E1p subunit of the pyruvate dehydrogenase complex (Buchholz et al., 2013), and activating the

glyoxylate shunt via guided evolution of isocitrate dehydrogenase in a phosphoenolpyruvate carboxylase- and pyruvate carboxylase-deficient mutant (Schwentner et al., 2018), dramatically improved L-valine overproduction in *C. glutamicum* without acetate supplementation. As such, we are currently exploring strategies to improve the performance of our L-valine-overproducing *B. subtilis* strains.

ORCID

C. Perry Chou http://orcid.org/0000-0002-7254-8118

REFERENCES

Belitsky, B. R. (2015). Role of branched-chain amino acid transport in *Bacillus subtilis* CodY activity. *Journal of Bacteriology*, *197*(8), 1330–1338.

Belitsky, B. R., & Sonenshein, A. L. (2011). Contributions of multiple binding sites and effector-independent binding to CodY-mediated regulation in *Bacillus subtilis*. *Journal of Bacteriology*, *193*(2), 473–484.

Belitsky, B. R., & Sonenshein, A. L. (2013). Genome-wide identification of *Bacillus subtilis* CodY-binding sites at single-nucleotide resolution. *Proceedings of the National Academy of Sciences of the United States of America*, *110*(17), 7026–7031.

Blombach, B., Schreiner, M. E., Bartek, T., Oldiges, M., & Eikmanns, B. J. (2008). *Corynebacterium glutamicum* tailored for high-yield L-valine production. *Applied Microbiology and Biotechnology*, *79*(3), 471–479.

Bott, M., & Eikmanns, B. J. (2013). TCA cycle and glyoxylate shunt of *Corynebacterium glutamicum*. In Yukawa, H., & Inui, M. (Eds.), *Corynebacterium glutamicum: Biology and biotechnology* (Vol. 23, pp. 281–313). Berlin: Springer.

Brinsmade, S. R., Alexander, E. L., Livny, J., Stettner, A. I., Segre, D., Rhee, K. Y., & Sonenshein, A. L. (2014). Hierarchical expression of genes controlled by the *Bacillus subtilis* global regulatory protein CodY. *Proceedings of the National Academy of Sciences of the United States of America*, *111*(22), 8227–8232.

Buchholz, J., Schwentner, A., Brunnenkan, B., Gabris, C., Grimm, S., Gerstmeir, R., … Blombach, B. (2013). Platform engineering of *Corynebacterium glutamicum* with reduced pyruvate dehydrogenase complex activity for improved production of L-lysine, L-valine, and 2-ketoisovalerate. *Applied and Environmental Microbiology*, *79*(18), 5566–5575.

Chen, C., Li, Y., Hu, J., Dong, X., & Wang, X. (2015). Metabolic engineering of *Corynebacterium glutamicum* ATCC13869 for L-valine production. *Metabolic Engineering*, *29*, 66–75.

Chipman, D., Barak, Z., Schloss, J. V., & Schloss, J. V. (1998). Biosynthesis of 2-aceto-2-hydroxy acids: Acetolactate synthases and acetohydroxyacid synthases. *Biochimica et Biophysica Acta*, *1385*(2), 401–419.

Debarbouille, M., Gardan, R., Arnaud, M., & Rapoport, G. (1999). Role of BkdR, a transcriptional activator of the SigL-dependent isoleucine and valine degradation pathway in *Bacillus subtilis*. *Journal of Bacteriology*, *181*(7), 2059–2066.

Elisakova, V., Patek, M., Holatko, J., Nesvera, J., Leyval, D., Goergen, J.-L., & Delaunay, S. (2005). Feedback-resistant acetohydroxy acid synthase increases valine production in *Corynebacterium glutamicum*. *Applied and Environmental Microbiology*, *71*(1), 207–213.

Errington, J. (2003). Regulation of endospore formation in *Bacillus subtilis*. *Nature Reviews Microbiology*, *1*(2), 117–126.

Fischer, E., & Sauer, U. (2005). Large-scale in vivo flux analysis shows rigidity and suboptimal performance of *Bacillus subtilis* metabolism. *Nature Genetics*, *37*(6), 636–640.

Fradrich, C., March, A., Fiege, K., Hartmann, A., Jahn, D., & Hartig, E. (2012). The transcription factor AlsR binds and regulates the promoter of the alsSD operon responsible for acetoin formation in *Bacillus subtilis*. *Journal of Bacteriology*, *194*(5), 1100–1112.

Fujita, Y., Satomura, T., Tojo, S., & Hirooka, K. (2014). CcpA-mediated catabolite activation of the *Bacillus subtilis* ilv-leu operon and its negation by either CodY-or TnrA-mediated negative regulation. *Journal of Bacteriology*, *196*(21), 3793–3806.

Grandoni, J. A., Fulmer, S. B., Brizzio, V., Zahler, S. A., & Calvo, J. M. (1993). Regions of the *Bacillus subtilis* ilv-leu operon involved in regulation by leucine. *Journal of Bacteriology*, *175*(23), 7581–7593.

Hartl, B., Wehrl, W., Wiegert, T., Homuth, G., & Schumann, W. (2001). Development of a new integration site within the *Bacillus subtilis* chromosome and construction of compatible expression cassettes. *Journal of Bacteriology*, *183*(8), 2696–2699.

Hasegawa, S., Suda, M., Uematsu, K., Natsuma, Y., Hiraga, K., Jojima, T., … Yukawa, H. (2013). Engineering of *Corynebacterium glutamicum* for high-yield L-valine production under oxygen deprivation conditions. *Applied and Environmental Microbiology*, *79*(4), 1250–1257.

Morabbi heravi, K., Wenzel, M., & Altenbuchner, J. (2011). Regulation of mtl operon promoter of *Bacillus subtilis*: Requirements of its use in expression vectors. *Microbial Cell Factories*, *10*(1), 83.

Johnson, M., Zaretskaya, I., Raytselis, Y., Merezhuk, Y., McGinnis, S., & Madden, T. L. (2008). NCBI BLAST: A better web interface. *Nucleic Acids Research*, *36*(Suppl. 2), W5–W9.

Kabisch, J., Pratzka, I., Meyer, H., Albrecht, D., Lalk, M., Ehrenreich, A., & Schweder, T. (2013). Metabolic engineering of *Bacillus subtilis* for growth on overflow metabolites. *Microbial Cell Factories*, *12*(1), 72.

Kaplun, A., Vyazmensky, M., Zherdev, Y., Belenky, I., Slutzker, A., Mendel, S., … Shaanan, B. (2006). Structure of the regulatory subunit of acetohydroxyacid synthase isozyme III from *Escherichia coli*. *Journal of Molecular Biology*, *357*(3), 951–963.

Karau, A., & Grayson, I. (2014). Amino acids in human and animal nutrition. In Zorn, H., & Czermak, P. (Eds.), *Biotechnology of food and feed additives* (Vol. 143, pp. 189–228). Berlin: Springer.

Krämer, R. (1994). Secretion of amino acids by bacteria: Physiology and mechanism. *FEMS Microbiology Reviews*, *13*(1), 75–93.

Kutukova, E. A., Livshits, V. A., Altman, I. P., Ptitsyn, L. R., Zyiatdinov, M. H., Tokmakova, I. L., & Zakataeva, N. P. (2005). The yeaS (leuE) gene of *Escherichia coli* encodes an exporter of leucine, and the Lrp protein regulates its expression. *FEBS Letters*, *579*(21), 4629–4634.

Leyval, D., Uy, D., Delaunay, S., Goergen, J. L., & Engasser, J. M. (2003). Characterisation of the enzyme activities involved in the valine biosynthetic pathway in a valine-producing strain of *Corynebacterium glutamicum*. *Journal of Biotechnology*, *104*(1-3), 241–252.

Li, S., Huang, D., Li, Y., Wen, J., & Jia, X. (2012). Rational improvement of the engineered isobutanol-producing *Bacillus subtilis* by elementary mode analysis. *Microbial Cell Factories*, *11*(1), 101.

Liu, L., Liu, Y., Li, J., Du, G., & Chen, J. (2011). Microbial production of hyaluronic acid: Current state, challenges, and perspectives. *Microbial Cell Factories*, *10*(1), 99.

Livshits, V. A., Doroshenko, V. G., Gorshkova, N. V., Belaryeva, A. V., Ivanovskaya, L. V., Khourges, E. M., … Kozlov, Y. I. 2004. Mutant ilvH gene and method for producing l-valine. Google Patents.

Lu, Z., Takeuchi, M., & Sato, T. (2007). The LysR-type transcriptional regulator YofA controls cell division through the regulation of expression of ftsW in Bacillus subtilis. *Journal of Bacteriology*, *189*, 5642–5651.

Mader, U., Hennig, S., Hecker, M., & Homuth, G. (2004). Transcriptional organization and posttranscriptional regulation of the *Bacillus subtilis* branched-chain amino acid biosynthesis genes. *Journal of Bacteriology*, *186*(8), 2240–2252.

Maloy, S. R., & Nunn, W. D. (1982). Genetic regulation of the glyoxylate shunt in *Escherichia coli*K-12. *Journal of Bacteriology*, *149*(1), 173–180.

Mendel, S., Elkayam, T., Sella, C., Vinogradov, V., Vyazmensky, M., Chipman, D. M., & Barak, Z. (2001). Acetohydroxyacid synthase: A proposed structure for regulatory subunits supported by evidence from mutagenesis. *Journal of Molecular Biology*, *307*(1), 465–477.

Molle, V., Nakaura, Y., Shivers, R. P., Yamaguchi, H., Losick, R., Fujita, Y., & Sonenshein, A. L. (2003). Additional targets of the *Bacillus subtilis* global regulator CodY identified by chromatin immunoprecipitation and genome-wide transcript analysis. *Journal of Bacteriology*, *185*(6), 1911–1922.

Oldiges, M., Eikmanns, B. J., & Blombach, B. (2014). Application of metabolic engineering for the biotechnological production of L-valine. *Applied Microbiology and Biotechnology*, *98*(13), 5859–5870.

Park, J. H., Jang, Y. S., Lee, J. W., & Lee, S. Y. (2011). *Escherichia coli* W as a new platform strain for the enhanced production of L-valine by systems metabolic engineering. *Biotechnology and Bioengineering*, *108*(5), 1140–1147.

Park, J. H., Kim, T. Y., Lee, K. H., & Lee, S. Y. (2011). Fed-batch culture of *Escherichia coli* for L-valine production based on in silico flux response analysis. *Biotechnology and Bioengineering*, *108*(4), 934–946.

Park, J. H., Lee, K. H., Kim, T. Y., & Lee, S. Y. (2007). Metabolic engineering of *Escherichia coli* for the production of L-valine based on transcriptome analysis and in silico gene knockout simulation. *Proceedings of the National Academy of Sciences of the United States of America*, *104*(19), 7797–7802.

Phan, T. T. P., Nguyen, H. D., & Schumann, W. (2012). Development of a strong intracellular expression system for *Bacillus subtilis* by optimizing promoter elements. *Journal of Biotechnology*, *157*(1), 167–172.

Qi, L. S., Larson, M. H., Gilbert, L. A., Doudna, J. A., Weissman, J. S., Arkin, A. P., & Lim, W. A. (2013). Repurposing CRISPR as an RNA-guided platform for sequence-specific control of gene expression. *Cell*, *152*(5), 1173–1183.

Radmacher, E., Vaitsikova, A., Burger, U., Krumbach, K., Sahm, H., & Eggeling, L. (2002). Linking central metabolism with increased pathway flux: L-Valine accumulation by *Corynebacterium glutamicum*. *Applied and Environmental Microbiology*, *68*(5), 2246–2250.

Rahmer, R., Morabbi heravi, K., & Altenbuchner, J. (2015). Construction of a super-competent *Bacillus subtilis* 168 using the PmtlA-comKS inducible cassette. *Frontiers in Microbiology*, *6*, 6.

Reents, H., Munch, R., Dammeyer, T., Jahn, D., & Hartig, E. (2006). The Fnr regulon of *Bacillus subtilis*. *Journal of Bacteriology*, *188*(3), 1103–1112.

Renna, M. C., Najimudin, N., Winik, L. R., & Zahler, S. A. (1993). Regulation of the *Bacillus subtilis* alsS, alsD, and alsR genes involved in post-exponential-phase production of acetoin. *Journal of Bacteriology*, *175*(12), 3863–3875.

Sambrook, J., & Russell, D. (2001). *Molecular cloning: A laboratory manual*. Cold Spring Harbor, NY: Cold Spring Harbor Laboratory Press.

Schallmey, M., Singh, A., & Ward, O. P. (2004). Developments in the use of *Bacillus* species for industrial production. *Canadian Journal of Microbiology*, *50*(1), 1–17.

Schwentner, A., Feith, A., Münch, E., Busche, T., Rückert, C., Kalinowski, J., … Blombach, B. (2018). Metabolic engineering to guide evolution–Creating a novel mode for L-valine production with *Corynebacterium glutamicum*. *Metabolic Engineering*, *47*, 31–41.

Sierro, N., Makita, Y., de Hoon, M., & Nakai, K. (2007). DBTBS: A database of transcriptional regulation in *Bacillus subtilis* containing upstream intergenic conservation information. *Nucleic Acids Research*, *36*(Suppl. 1), D93–D96.

Sonenshein, A. L. (2007). Control of key metabolic intersections in *Bacillus subtilis*. *Nature Reviews Microbiology*, *5*(12), 917–927.

Tojo, S., Satomura, T., Morisaki, K., Yoshida, K.-I., Hirooka, K., & Fujita, Y. (2004). Negative transcriptional regulation of the ilv-leu operon for biosynthesis of branched-chain amino acids through the *Bacillus subtilis* global regulator TnrA. *Journal of Bacteriology*, *186*(23), 7971–7979.

Ulusoy, S., Ulusoy, H. I., Pleissner, D., & Eriksen, N. T. (2016). Nitrosation and analysis of amino acid derivatives by isocratic HPLC. *RSC Advances*, *6*(16), 13120–13128.

Westbrook, A. W., Moo-Young, M., & Chou, C. P. (2016). Development of a CRISPR-Cas9 tool kit for comprehensive engineering of *Bacillus subtilis*. *Applied and Environmental Microbiology*, *82*(16), 4876–4895.

Westbrook, A. W., Ren, X., Moo-Young, M., & Chou, C. P. (2018). Engineering of cell membrane to enhance heterologous production of hyaluronic acid in *Bacillus subtilis*. *Biotechnology and Bioengineering*, *115*(1), 216–231.

Westbrook, A. W., Ren, X., Oh, J., Moo-Young, M., & Chou, C. P. (2018). Metabolic engineering to enhance heterologous production of hyaluronic acid in *Bacillus subtilis*. *Metabolic Engineering*, *47*, 401–413.

Westers, L., Westers, H., & Quax, W. J. (2004). *Bacillus subtilis* as cell factory for pharmaceutical proteins: A biotechnological approach to optimize the host organism. *Biochimica et Biophysica Acta*, *1694*(1–3), 299–310.

Wolf, M., Geczi, A., Simon, O., & Borriss, R. (1995). Genes encoding xylan and β-glucan hydrolysing enzymes in *Bacillus subtilis*: Characterization, mapping and construction of strains deficient in lichenase, cellulase and xylanase. *Microbiology*, *141*(2), 281–290.

Xie, N.-Z., Liang, H., Huang, R.-B., & Xu, P. (2014). Biotechnological production of muconic acid: Current status and future prospects. *Biotechnology Advances*, *32*(3), 615–622.

Yang, T., Rao, Z., Kimani, B. G., Xu, M., Zhang, X., & Yang, S.-T. (2015). Two-step production of gamma-aminobutyric acid from cassava powder using *Corynebacterium glutamicum* and *Lactobacillus plantarum*. *Journal of Industrial Microbiology & Biotechnology*, *42*(8), 1157–1165.

Yoneda, T, Miyota, Y, Furuya, K, Tsuzuki, T. 2006. Production process of surfactin. Google Patents.

Zamboni, N., Fischer, E., Muffler, A., Wyss, M., Hohmann, H. P., & Sauer, U. (2005). Transient expression and flux changes during a shift from high to low riboflavin production in continuous cultures of *Bacillus subtilis*. *Biotechnology and Bioengineering*, *89*(2), 219–232.

Zhang, K., Duan, X., & Wu, J. (2016). Multigene disruption in undomesticated *Bacillus subtilis* ATCC 6051a using the CRISPR/Cas9 system. *Scientific Reports*, *6*, 27943.

SUPPORTING INFORMATION

Additional supporting information may be found online in the Supporting Information section at the end of the article.

How to cite this article: Westbrook AW, Ren X, Moo-Young M, Chou CP. Metabolic engineering of *Bacillus subtilis* for L-valine overproduction. *Biotechnology and Bioengineering*. 2018;115:2778–2792. https://doi.org/10.1002/bit.26789